Optica Applicata, Vol. XLIII, No. 4, 2013
DOI: 10.5277/oa130404

The effect of fluorine and tungsten co-doping on optical, electrical and structural properties of tin (IV) oxide thin films prepared by sol–gel spin coating method

EYÜP FAHRI KESKENLER[1*], GÜVEN TURGUT[2], SERDAR AYDIN[2], SEYDI DOGAN[3], BAHATTIN DUZGUN[2]

[1]Recep Tayyip Erdogan University, Faculty of Engineering, Department of Nanotechnology Engineering, 53100 Rize, Turkey

[2]Ataturk University, K.K. Education Faculty, Department of Physics, 25250 Erzurum, Turkey

[3]Balikesir University, Faculty of Engineering and Architecture, Department of Electrical and Electronics Engineering, 10145 Balikesir, Turkey

[*]Corresponding author: keskenler@gmail.com

Fluorine and tungsten co-doped tin (IV) oxide (WFTO) thin films have been prepared first time by a sol–gel spin coating method. The effect of F and W co-dopant ratio on optical, electrical and structural properties of SnO_2 was investigated. It was found that the optical properties of the films were obviously affected by the co-dopant ratio. When the F:W co-dopant ratio increases from 0.25:0.25 to 0.75:0.50, the transmittance in the short wavelengths slightly increases and transmittance edge shifts towards shorter wavelength. With an increase in the co-dopant ratio, the reduction and red shifts in the optical transmittance edge are very obvious at all wavelengths. Transmittance values at 550 nm for the films have varied between 79.64% and 50.20%. The indirect and direct band gap values for WFTO-1, WFTO-2, WFTO-3 and WFTO-4 samples were calculated to be 3.73, 3.79, 3.48, 3.40 eV and 4.03, 4.04, 3.98, 3.97 eV, respectively. The crystal structure of the films has been investigated by X-ray diffraction patterns. It has been observed that WFTO-1 and WFTO-2 samples have (111) preferential orientation corresponding to SnO_2 cubic phase. This orientation almost disappears and changes to tetragonal phase (110) orientation for WFTO-3 and WFTO-4. To the best of our knowledge, this is the first cubic structure observation for SnO_2 grown by the sol–gel technique. The electrical properties were also changed with co-doping ratio. The best optical, electrical and structural properties were obtained for mole ratio 0.75:0.50 (F:W).

Keywords: tin (IV) oxide (SnO_2), fluorine (F) and tungsten (W) co-doping, sol–gel.

1. Introduction

Transparent and conductive thin films, owing to their high transmittance and conductivity, have widely been used in optoelectronic applications [1, 2]. In recent years, there has been a growing interest in the use of transparent conducting oxide thin

films for the conducting solar window materials [3], heat reflectors [4, 5] and various gas sensors [6, 7] and their applications. Among the different transparent conductive oxides, tin (IV) oxide (SnO_2) has significant commercialization [8, 9]. When SnO_2 is co-doped with F and W, the dopants give extra free electrons to SnO_2 lattice [10, 11] and cause an increase in the electrical conductivity and optical transmittance. Both parameters make films more appropriate for solar cell application. Doped and undoped SnO_2 thin films can be synthesized by various techniques such as thermal evaporation [8], sputtering [12], chemical vapor deposition [13], spray pyrolysis [11], hydrothermal method [14], pulsed plasma deposition (PPD) [15], pulsed laser deposition (PLD) [16], reactive evaporation [17] and the sol–gel spin coating technique [18]. Among these techniques, the sol–gel spin coating is attractive due to its easy manipulation, ability to prepare high quality thin films in a large scale, simplicity, safety, low cost of apparatus [19–21] and easy control of chemical components [22]. To the best of our knowledge, the synthesis of F and W co-doped SnO_2 films has not been reported up to now by the sol–gel spin coating method. Therefore, in this study, we aimed to investigate the effect of F and W co-doping on optical, electrical and structural properties of spin coated SnO_2 films. Also, we investigated the evaluation of these films for use as a transparent conductor material in solar cell applications.

2. Experiment

2.1. Sample preparation

In the present study, F and W co-doped tin oxide (WFTO) films were prepared by the sol–gel spin coating method on soda lime glass substrates having about 5 eV band gap value [23]. The precursor solution was prepared by using tin chloride dihydrate ($SnCl_2 \cdot 2H_2O$), 2-methoxyethanol ($C_3H_8O_2$) and monoethanolamine (C_2H_7NO, MEA) as starting material, solvent and stabilizer, respectively. For the F and W co-doped thin films, ammonium fluoride (NH_4F) and tungsten hexachloride (WCl_6) form were used as fluorine and tungsten doping source, respectively, and they simultaneously were added by dissolving in the solution. The molar ratios of $SnCl_2 \cdot 2H_2O$ and metal dopant sources to MEA were maintained at 1:1. 0.1 M $SnCl_2 \cdot 2H_2O$, 0.1 M NH_4F and 0.1 M WCl_6 were mixed in different solutions to obtain the mole ratios as 0.25:0.25, 0.75:0.50, 1.25:0.75, 1.75:1.00 for F and W, respectively. The co-doped films were named as WFTO-1, WFTO-2, WFTO-3 and WFTO-4, respectively. The precursor sol was stirred at 70 °C for 1 h in a tightly-closed flask to obtain a clear and homogenous solution. Soda-lime glass substrates were kept in boiling chromic acid solution and they were rinsed with deionized water. They then were cleaned with acetone, methanol and deionized water by using an ultrasonic cleaner and dried with nitrogen. The substrate dropped resultant solution was rotated at a speed of 2500 rpm for 30 s by using a spin-coater. After the glass substrates were coated, they were sintered at 200 °C for 5 min to evaporate solvent and remove the organic sediments and then spontaneously cooled to room temperature. This procedure was repeated for seven times and finally the samples were annealed in air ambient at 450 °C for 30 min.

2.2. Characterization

The optical transmittance and absorbance measurements were recorded in the spectral region of 300–1000 nm at 300 K by using a UV-VIS spectrophotometer (Perkin–Elmer, Lambda 40) which works in the range of 200–1100 nm. When the optical properties of the films were measured, a soda-lime glass being identical to substrate was used as a reference. Therefore, transmittance and absorbance values of glass substrate without a film were extracted from the values obtained for the deposited film grown on a substrate at the same wavelength; and therefore, only the transmittance and absorbance of the films were obtained. The structural characterization of the WFTO thin films was carried out by X-ray diffraction (XRD) measurements using a Rigaku Miniflex II diffractometer with CuKα radiation ($\lambda = 1.5418$ Å). The diffractometer reflections were taken at room temperature and the values of 2θ were altered between 10 and 80 deg in step of 0.05 deg.The sheet resistance values of films were measured by means of the four point probe technique by using Keithley 2400 sourcemeter. In four probe measurements, probes were arranged in a single line and outer pair was carrying current and the sheet resistance values were obtained from values of applied current and measured voltage (by measuring voltage between inner pairs).

3. Results and discussions

3.1. Optical properties

The optical properties of WFTO thin films were investigated by UV-VIS spectrometer at room temperature. The transmittance spectra of the films have been given in Fig. 1. As can be seen from this figure, when the F/W co-dopant ratio increases from 1.00 for WFTO-1 to 1.50 for WFTO-2, the transmittance in the short wavelengths slightly increases. Compared with WFTO-1, the optical transmittance edge of the WFTO-2 shifts slightly towards shorter wavelength. With the increase in the co-dopant ratio, 1.66 for WFTO-3 and 1.75 for the WFTO-4, the reduction and red shifts in the optical trans-

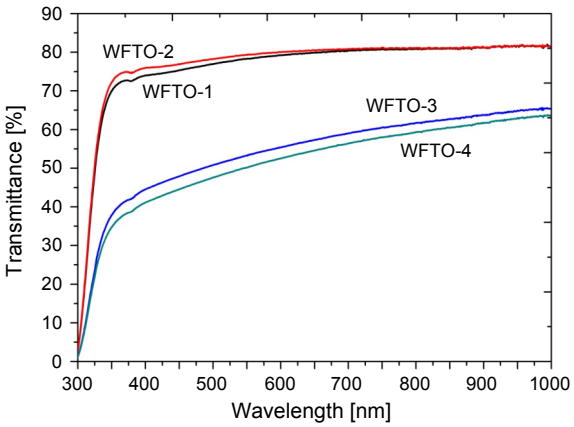

Fig. 1. The optical transmittance spectra for WFTO thin films.

mittance edge are very obvious at all wavelength ranges. The reason of the decrease in transmittance at a higher dopant ratio (or doping concentration) may be defects being created by high doping.

The analysis of the dependence of an absorption coefficient on photon energy in the high absorption regions is carried out to obtain the detailed information about the energy band gaps. The absorption coefficient α is determined by the Lambert's equation [24],

$$\alpha = \frac{\ln(1/T)}{d} \tag{1}$$

where T is the transmittance and d is the film thickness. The variation of the absorption coefficient against the photon energy $h\nu$ has the form of [25]

$$\alpha h\nu = A(h\nu - E_g)^{n/2} \tag{2}$$

where E_g is the band gap, A is a constant and n is equal to one for a direct-gap material and to four for an indirect-gap material [26]. To determine whether the co-doped films have a direct or indirect band gap, $(\alpha h\nu)^2$ *vs*. photon energy and $(\alpha h\nu)^{1/2}$ *vs*. photon energy figures were attempted to plot and these plots were given in Figs. 2 and 3, respectively. In addition, the inset of Fig. 3 shows the band gap energy determination of samples for smaller scale axis because of separating lines. As can be seen from squares indicated by red lined in these figures, the $(\alpha h\nu)^2$ *vs*. photon energy plots have better linearity than $(\alpha h\nu)^{1/2}$ *vs*. photon energy plots. Therefore, it can be concluded that the co-doped films are direct band gap semiconductor materials [26]. The indirect and direct band gap values for WFTO-1, WFTO-2, WFTO-3 and WFTO-4 samples were calculated to be 3.73, 3.79, 3.48, 3.40 eV and 4.03, 4.04, 3.98, 3.97 eV,

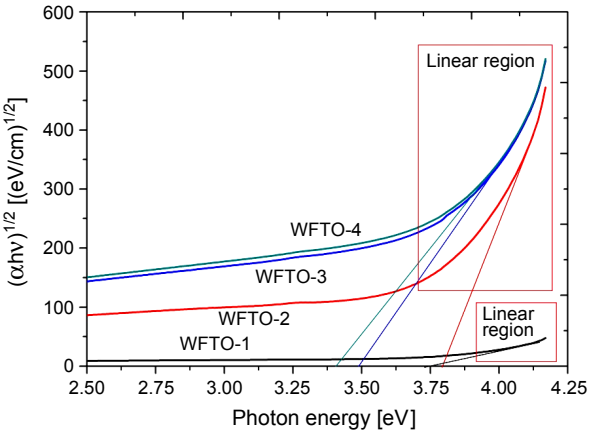

Fig. 2. The $(\alpha h\nu)^{1/2}$ *versus* photon energy plot for the calculation of an indirect band gap value of WFTO samples.

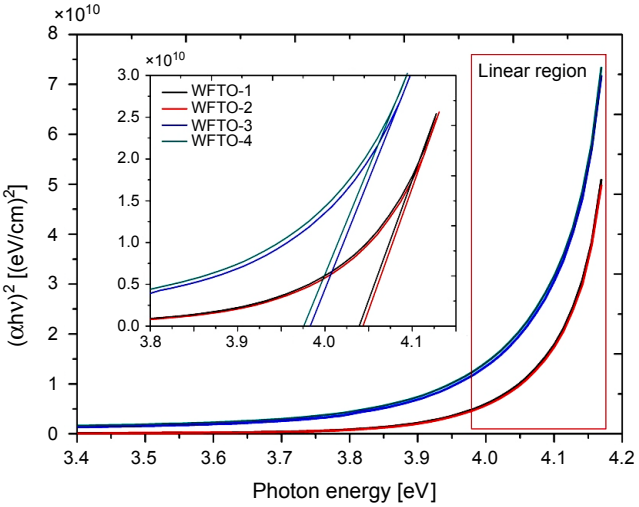

Fig. 3. The $(\alpha h\nu)^2$ *versus* photon energy plot for the calculation of a direct band gap of WFTO samples; the inset shows the band gab energy determination of samples for smaller scale axis because of separating lines.

respectively. As can be expected, the direct optical band gap values are higher compared to indirect optical band gap values. The similar results were obtained by Dua *et al*. [27] and the direct optical band gap values agree with those found by Dua *et al*. [27] and Th Diana *et al*. [28].

When F and W co-dopant ratio is increased from 0.25:0.25 (F:W) for WFTO-1 to 0.75:0.50 for WFTO-2 in SnO_2 lattice, the band gap value slightly increases and then decreases with further F and W co-dopant ratios. The reason of the increase in the band gap with W and F co-doping can probably be explained as follows; since SnO_2 is one of degenerate semiconductors [29] in which the Fermi level is within the conduction band [30], the optical band gaps are directly related to the excitation of the electrons from the valance band to Fermi level [31, 32] and/or conduction band. This means that there is a shift of the Fermi level into the conduction band of the semiconductor due to the increase in the carrier density leading to the energy band broadening (shifting) with some of the Sn^{4+} and O^{2-} ions being replaced by W^{6+} and F^- in the lattice. This is called the Moss–Burstein effect [33]. As can be seen from XRD spectra of the films, the decrease in the peak intensities can be attributed to the crystal quality being deteriorated with a co-doping ratio increase. When F and W co-doping ratio is increased in the crystal structure, the dopants cannot be placed into the proper lattice positions. This can lead to forming crystal defects and causing high surface roughness. Therefore, the decrease in the band gap and transmittance values for WFTO-3 and WFTO-4 films can be due to the enhancement in photon scattering because of crystal defects which create lattice strain by co-doping with F and W [34–36].

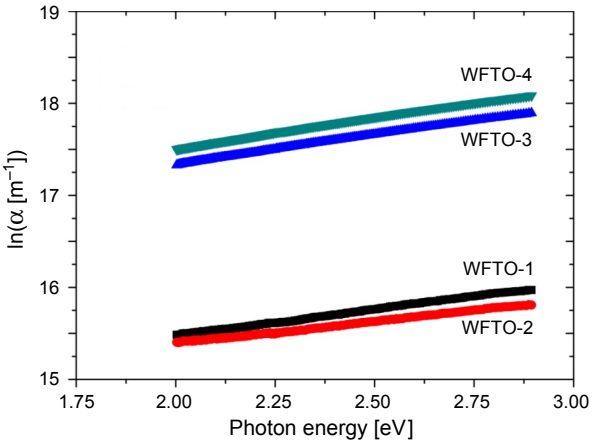

Fig. 4. The Urbach plots for the WFTO films.

Exponential absorption tails for photon energies of sub-band gap in both crystalline and amorphous materials have attracted considerable attention in recent years. Various mechanisms such as the excitons may affect the absorption phenomena. Figure 4 shows spectral dependences of the logarithm of an absorption coefficient as a function of energy for WFTO films.

The optical absorption coefficient shows a temperature-dependent exponential tail for $E < E_g$ [37]:

$$\alpha(E, T) = \alpha_0 \exp\left\{\frac{E - E_0}{E_u(T, X)}\right\} \tag{3}$$

where, E_0 and α_0 are constants, which can be determined from the $\ln(\alpha)$ *versus* E. Urbach energy E_u is assigned to the steepness of the Urbach tail. It is a function of temperature and the degree of crystal disorder of the material. It has a significant role in the characteristic analysis of a semiconductor. The previous statements imply that the Urbach energy can be expressed into two components as a temperature-dependent and temperature-independent term:

$$E_u(T, X) = E_u(T) + E_u(X) \tag{4}$$

The thermal disorder of the material is associated with the temperature-dependent term, while the temperature-independent component is related to its inherent structural disorder [38]. The steepness parameter σ is found as:

$$\sigma = \frac{kT}{E_u} \tag{5}$$

By taking the natural logarithm on both sides of Eq. (5):

$$\ln(\alpha) = \frac{E}{E_u}\left[\ln(\alpha_0) + \frac{E_0}{E_u}\right] \tag{6}$$

where Urbach energy E_u is equal to the absorption edge energy width and inverse to the absorption edge slope value,

$$E_u^{-1} = \frac{\mathrm{d}\left[\ln(\alpha)\right]}{\mathrm{d}E} \tag{7}$$

where Urbach energy E_u only depends on the degree of structural disorders as a function of X (lattice strains and dislocation densities), in constant temperature [38].

The E_u values were found to be 140, 141, 158 and 160 meV and σ values were found to be 1.846×10^{-4}, 1.833×10^{-4}, 1.636×10^{-4} and 1.617×10^{-4} for WFTO-1, WFTO-2, WFTO-3 and WFTO-4, respectively. Urbach energy values of the films increase with F/W co-dopant ratio. The optical band gaps of the films change oppositely with Urbach energy. This result causes a redistribution of states, such as from band-to-tail and tail-to-tail transitions, and the optical gap decreases due to the broadening of the Urbach tail.

The reflectance R of the films is found by using relationship [39],

$$R + T + A = 1 \tag{8}$$

where T and A are transmission and absorption, respectively. The absorption and reflectance (as a percentage) spectra are given in Figs. 5 and 6, respectively. Refractive index n of the samples and extinction coefficient k are calculated by the following equations [40]:

$$n = \frac{1+R}{1-R} + \sqrt{\frac{4R}{(1-R)^2} - k^2} \tag{9}$$

and

$$k = \frac{\alpha\lambda}{4\pi} \tag{10}$$

where R, α and λ are reflectance, absorption coefficient and wavelength, respectively. The n and k values dependence on wavelength is shown in Figs. 7 and 8, respectively.

As can be seen from Figs. 7 and 8, n and k values depend on wavelength. Compared with WFTO-1, the extinction coefficient value of WFTO-2 decreases for WFTO-2 and then continuously increases with the increase in the W/F co-dopant ratio for WFTO-3 and WFTO-4. At short wavelengths, k values are small due to the Burstein–Moss shift [33], but they are high at near-infrared spectral regions

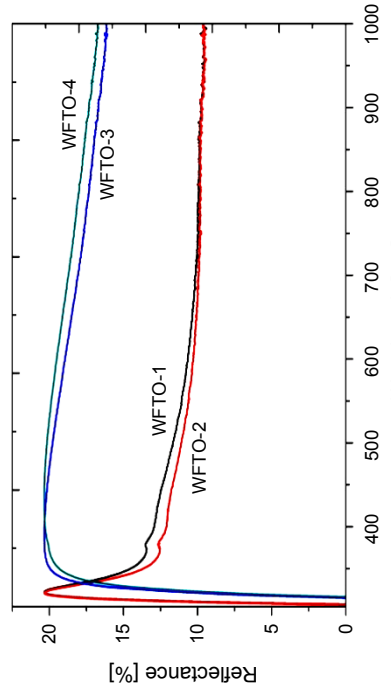

Fig. 6. The reflectance spectra for the WFTO thin films.

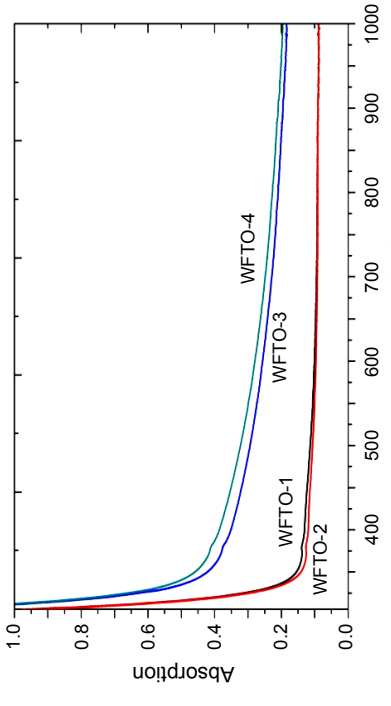

Fig. 5. The absorption spectra for the WFTO thin films.

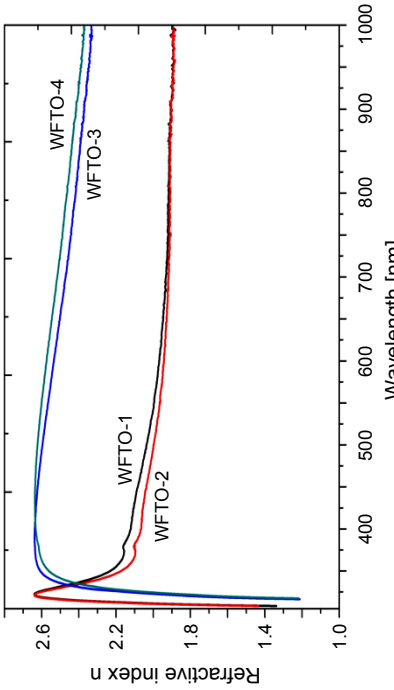

Fig. 8. The variation of refractive index for WFTO thin films with wavelength.

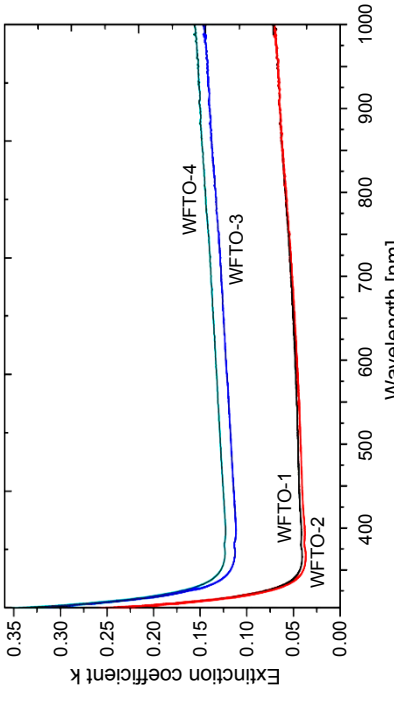

Fig. 7. The variation of extinction coefficient with wavelength for WFTO thin films.

because of the increase in the free carrier absorption [41]. The n values have been obtained for the different W/F co-dopant ratio, and their average values for WFTO-1, WFTO-2, WFTO-3 and WFTO-4 were found to be 1.99, 1.98, 2.48 and 2.51, respectively. These values are in agreement with those reported by other researchers [42–44]. It can be concluded that the films with lower carrier concentration have a higher refractive index. The values of the refractive index in this study are comparable to those reported in the literature [45, 46].

The fundamental electron excitation spectrum of the films is described by means of a complex electronic dielectric constant. The real ε_1 and imaginary ε_2 parts of the dielectric constant are related to the n and k values. The ε_1 and ε_2 values are calculated using the following equations [47, 48]:

$$\varepsilon_1 = n^2 - k^2 \tag{11}$$

$$\varepsilon_2 = 2nk \tag{12}$$

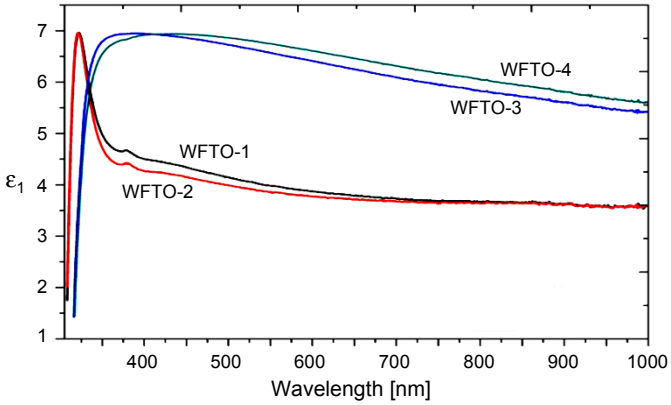

Fig. 9. The variation of real dielectric constants for WFTO films as a function of wavelength.

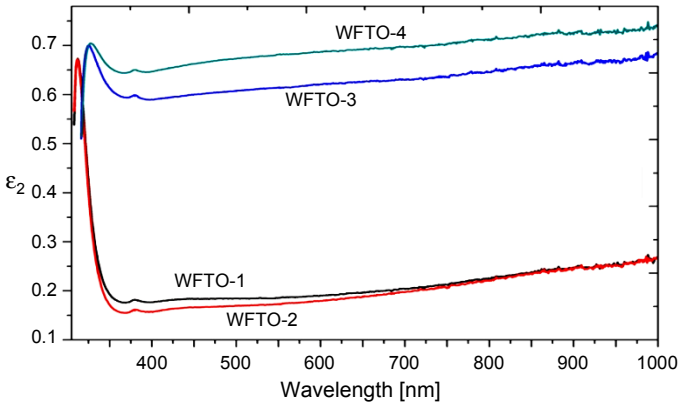

Fig. 10. The variation of imaginary dielectric constants for WFTO films as a function of wavelength.

The dielectric constant values depending on the wavelength have been given in Figs. 9 and 10, respectively. As can be seen in these figures, the ε_1 values are higher than ε_2 values.

3.2. Electrical properties

The sheet resistance values of WFTO films were measured by a four point probe method. As can be seen in Tab. 1, the F/W co-dopant ratio increases from 1.00 for WFTO-1 to 1.50 for WFTO-2, there is a decrease in sheet resistance, then there is a reduction in sheet resistance value for WFTO-3 (F/W ratio, 1.66) and WFTO-4 (F/W ratio, 1.75). The variation in the sheet resistance of SnO_2 with F and W co-doping

T a b l e 1. Optical and electrical properties of WFTO thin films.

Sample name	Sheet resistance R_s [Ω]	Band gap E_g [eV]	Transmittance T at 550 nm [%]	Figure of merit Φ [Ω^{-1}]
WFTO-1	14.50×10^4	4.03	78.27	5.95×10^{-7}
WFTO-2	8.61×10^4	4.04	79.64	1.19×10^{-6}
WFTO-3	11.30×10^4	3.98	53.28	1.63×10^{-8}
WFTO-4	13.10×10^4	3.97	50.20	7.76×10^{-9}

can be explained as follows: when SnO_2 is doped with F and W, some of the O^{2-} and Sn^{4+} ions in the lattice can be replaced by F^- and W^{6+} and this can cause the sheet resistance. In particular, a part of the W^{6+} ions is reduced to the low valance states, resulting in the formation of acceptor states and a loss of carriers [10, 15, 18]. In addition to this, F^- ions do not occupy suitable lattice states. Thus, the increase in the sheet resistance may be observed [11]. This result is in accordance with that of optical studies.

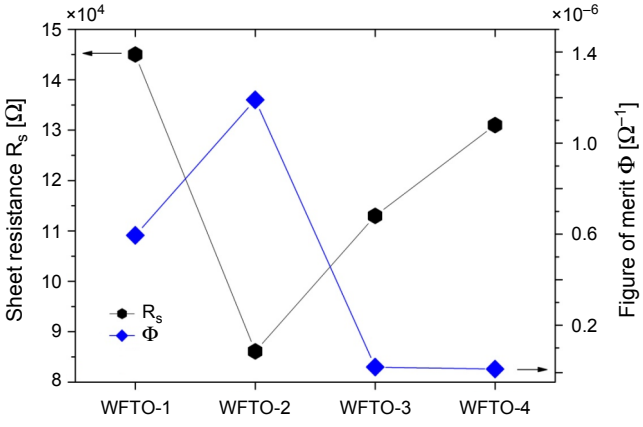

Fig. 11. Sheet resistance and figure of merit variation with W and F co-doping.

The figure of merit is an important parameter for evaluating transparent conducting oxides thin films for use in solar cells [31]. Therefore, the figure of merit values of the films was calculated and its variation with F/W co-dopant ratio was investigated. In order to compare the performance of various transparent conductors, the most widely used figure of merit is defined by the Haacke formulation [36],

$$\Phi = T^{10}/R_s \tag{13}$$

where T is the transmittance at 550 nm and R_s is the sheet resistance. This formula gives more weight to the transparency and thus is better adapted to solar cell technology. It is clear that figure of merit is dependent on the sheet resistance. Figure 11 shows the sheet resistance and figure of merit variation with F/W co-dopant ratio. The calculated figure of merit values are given in Table 1 together with sheet resistance, transmittance and band gap. It is found that WFTO-2 film has the highest value obtained in the present study (1.19×10^{-6} Ω^{-1}). This is possibly due to formation of a good quality film in terms of conductivity and transmittance.

3.3. Structural properties

The crystal structure of spin coated WFTO thin films has been investigated by X-ray diffraction (XRD) patterns. Figure 12 shows XRD spectra of F and W co-doped SnO_2 thin films. As can be seen from these spectra, WFTO-1 and WFTO-2 samples have (111) preferential orientation corresponding to SnO_2 cubic phase (JCPDS 50-1429), but this orientation almost disappears and changes to tetragonal phase (110) orientation (JCPDS 41-1445) for WFTO-3 and WFTO-4. To the best of our knowledge, this is the first cubic structure observation for SnO_2 grown by sol–gel technique. In the literature, generally ethanol [49, 50], 1-propyl alcohol [51], mixture of water and alco-

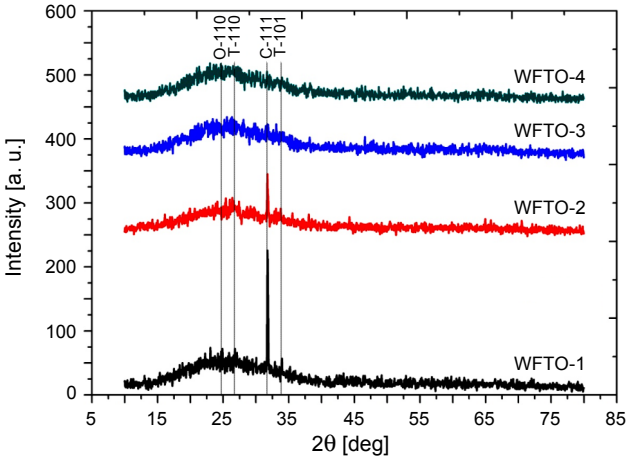

Fig. 12. XRD spectra for WFTO thin films.

hol [27, 52] are used as a solvent for the preparation of SnO_2 by the sol–gel route. YANWEI HUAN *et al*. [18] have prepared W-doped SnO_2 thin film from sol–gel solution including diluted $SnCl_2 \cdot 2H_2O$ and WCl_6 solved in the mixture of ethanol/water. SnO_2 tetragonal phase was obtained in all these studies. The (110) and (101) peaks of tetragonal phase have been observed at very little intensities for films. Also, there is an orthorhombic (110) peak (JCPDS 29-1484) at intensities which may be neglected. When the doping ratio is increased, it is observed that peak intensities continuously decrease and there is a nearly amorphous phase formation for WFTO-3 and WFTO-4. The reason for this may be that F and W atoms do not occupy the appropriate lattice sites with increasing doping and so crystallization deteriorates. SnO_2 crystallizes in the tetragonal rutile crystal system, but there are also orthorhombic and cubic phases of SnO_2. Tetragonal, orthorhombic and cubic phases of SnO_2 have been observed by some research groups [53, 54]. Similarly, in this study, SnO_2 hetero-phase structure has been observed.

4. Conclusions

In the present study, we have firstly prepared F and W co-doped SnO_2 thin films by the sol–gel spin coating method. The effect of F/W co-dopant ratio on optical properties of SnO_2 has extensively been investigated. Transmittances at 550 nm and optical band gap values for the films have varied between 79.64–50.20% and 4.04–3.97 eV, respectively, and the highest value was obtained for WFTO-2. The average refractive index values of WFTO-1, WFTO-2, WFTO-3 and WFTO-4 have been found to be 1.99, 1.98, 2.48 and 2.51, respectively. The electrical and structural properties of the films have also been investigated. It has been found that the co-dopant ratio is much effective on the optical and structural properties of the films. The best optical, electrical and structural properties were obtained for mole ratio 0.75:0.50 (F:W).

Acknowledgments – This work was supported by the Atatürk University Research Fund, Project Numbers: 2012/282 and 2012/283. One of the authors (G. Turgut) would like to thank Prof. Dr. Ümit Turgut and Assoc. Prof. Refik Dilber for their technical support.

References

[1] DENGKUI MIAO, QINGNAN ZHAO, SHUO WU, ZHENDONG WANG, XINGLIANG ZHANG, XIUJIAN ZHAO, *Effect of substrate temperature on the crystal growth orientation of SnO_2:F thin films spray-deposited on glass substrates*, Journal of Non-Crystalline Solids **356**(44–49), 2010, pp. 2557–2561.

[2] EXARHOS G.J., XIAO-DONG ZHOU, *Discovery-based design of transparent conducting oxide films*, Thin Solid Films **515**(18), 2007, pp. 7025–7052.

[3] ELANGOVAN E., RAMAMURTHI K., *Optoelectronic properties of spray deposited SnO_2:F thin films for window materials in solar cells*, Journal of Optoelectronics and Advanced Materials **5**(1), 2003, pp. 45–54.

[4] FRANK G., KAUER E., KÖSTLIN H., SCHMITTE F.J., *Transparent heat-reflecting coatings for solar applications based on highly doped tin oxide and indium oxide*, Solar Energy Materials **8**(4), 1983, pp. 387–398.

[5] COHEN S., *Low emissivity coatings for the improvement of the insulation properties of double-glazing units*, Thin Solid Films **77**(1–3), 1981, p. 127.
[6] GOETZBERGER A., HEBLING C., *Photovoltaic materials, past, present, future*, Solar Energy Materials and Solar Cells **62**(1–2), 2000, pp. 1–19.
[7] THANGARAJU B., *Structural and electrical studies on highly conducting spray deposited fluorine and antimony doped SnO_2 thin films from $SnCl_2$ precursor*, Thin Solid Films **402**(1–2), 2002, pp. 71–78.
[8] WAN-YOUNG CHUNG, CHANG-HYUN SHIM, DUK-DONG LEE, SOON-DON CHOI, *Tin oxide microsensor for LPG monitoring*, Sensors and Actuators B **20**(2–3), 1994, pp. 139–143.
[9] ELANGOVAN E., SHIVASHANKAR S.A., RAMAMURTHI K., *Studies on structural and electrical properties of sprayed SnO_2:Sb films*, Journal of Crystal Growth **276**(1–2), 2005, pp. 215–221.
[10] YANWEI HUANG, QUN ZHANG, GUIFENG LI, *Transparent conductive tungsten-doped tin oxide polycrystalline films prepared on quartz substrates*, Semiconductor Science and Technology **24**(1), 2009, article 015003.
[11] MOHOLKAR A.V., PAWAR S.M., RAJPURE K.Y., ALMARI S.N., PATIL P.S., BHOSALE C.H., *Solvent--dependent growth of sprayed FTO thin films with mat-like morphology*, Solar Energy Materials and Solar Cells **92**(11), 2008, pp. 1439–1444.
[12] QING NAN ZHAO, SHUO WU, DENG KUI MIAO, *Effect of substrate temperature on the haze and properties of SnO_2:F thin film coated on glass (FTO) by spray pyrolysis process*, Advanced Materials Research **150–151**, 2010, pp. 1043–1048.
[13] SHEWALE P.S., PATIL S.I., UPLANE M.D., *Preparation of fluorine-doped tin oxide films at low substrate temperature by an advanced spray pyrolysis technique, and their characterization*, Semiconductor Science and Technology **25**(11), 2010, article 115008.
[14] QIANWANG CHEN, YITAI QIAN, ZUYAO CHEN, GUIEN ZHOU, YUHENG ZHANG, *Fabrication of ultrafine SnO_2 thin films by the hydrothermal method*, Thin Solid Films **264**(1), 1995, pp. 25–27.
[15] HUANG Y., ZHANG Q., LI G., YANG M., *Tungsten-doped tin oxide thin films prepared by pulsed plasma deposition*, Materials Characterization **60**(5), 2009, pp. 415–419.
[16] NAKAO S., YAMADA N., HITOSUGI T., HIROSE Y., SHIMADA T., HASEGAWA T., *Fabrication of transparent conductive W-doped SnO_2 thin films on glass substrates using anatase TiO_2 seed layers*, Physica Status Solidi (C) **8**(2), 2011, pp. 543–545.
[17] MURANAKA S., BAND Y., *Reactive deposition of W-, Mo- and V-doped SnO_2 films*, Bulletin of the Institute for Chemical Research, Kyoto University **70**(4), 1992, pp. 430–434.
[18] YANWEI HUANG, DEZENG LI, JIAHAN FENG, GUIFENG LI, QUN ZHANG, ZHANG Q., *Transparent conductive tungsten-doped tin oxide thin films synthesized by sol–gel technique on quartz glass substrates*, Journal of Sol–Gel Science and Technology **54**(3), 2010, pp. 276–281.
[19] GHODSI F.E., ABSALAN H., *Comparative study of ZnO thin films prepared by different sol–gel route*, Acta Physica Polonica A **118**(4), 2010, pp. 659–664.
[20] SAGAR P., KUMAR M., MEHRA R.M., *Electrical and optical properties of sol–gel derive ZnO:Al thin films*, Materials Science-Poland **23**(3), 2005, pp. 685–696.
[21] ROKNABADI M. R., BEHDANI M., ARABSHAHI H., HODEINI N., *Indium-doped zinc oxide thin films sol–gel method*, International Review of Physics **12**, 2009, pp. 153–157.
[22] ILICAN S., CAGLAR Y., CAGLAR M., *Preparation and characterization of ZnO thin films deposited by sol–gel spin coating method*, Journal of Optoelectronics and Advanced Materials **10**, 2008, pp. 2578–2583.
[23] FARSON D.F., HAE WOON CHOI, ZIMMERMAN B. , STEACH J.K., CHALMERS J.J., OLESIK S.V., LEE L.J., *Femtosecond laser micromachining of dielectric materials for biomedical applications*, Journal of Micromechanics and Microengineering **18**(3), 2008, article 035020.
[24] SERIN T., SERIN N., KARADENIZ S., SARI H., TUGLUOGLU N., PAKMA O., *Electrical, structural and optical properties of SnO_2 thin films prepared by spray pyrolysis*, Journal of Non-Crystalline Solids **352**(3), 2006, pp. 209–215.

[25] TAUC J., GRIGOROVICI R., VANCU A., *Optical properties and electronic structure of amorphous germanium*, Physica Status Solidi (B) **15**(2), 1966, pp. 627–637.
[26] RAVICHANDRAN,K., MURUGANANTHAM G., SAKTHIVEL B., PHILOMINATHAN P., *Nanocrystalline doubly doped tin oxie films deposited using a simplified and low-cost spray technique for solar cell applications*, Journal of Ovonic Research **5**(3), 2009, pp. 63–69
[27] DUA L.K., DE A, CHAKRABORTY S., BISWAS P.K., *Study of spin coated high antimony content Sn–Sb oxide films on silica glass*, Materials Characterization **59**(5), 2008, pp. 578–586.
[28] TH DIANA, NOMITA DEVI K., NANDAKUMAR SARMA H., *On the optical properties of SnO_2 thin films prepared by sol–gel method*, Indian Journal of Physics **84**(6), 2010, pp. 687–691.
[29] BATZILL M., DIEBOLD U., *The surface and materials science of tin oxide*, Progress in Surface Science **79**(2–4), 2005, pp. 47–154.
[30] LINGANE J.J., SMALL L.A., *Polarography of the various oxidation states of tungsten*, Journal of American Chemical Society **71**(3), 1949, pp. 973–978.
[31] BABAR A.R., SHINDE S.S., MOHOLKAR A.V., BHOSALE C.H., KIM J.H., RAJPURE K.Y., *Structural and optoelectronic properties of antimony incorporated tin oxide thin films*, Journal of Alloys and Compounds **505**(2), 2010, pp. 416–422.
[32] BABAR A.R., SHINDE S.S., MOHOLKAR A.V., BHOSALE C.H., KIM J.H., RAJPURE K.Y., *Sensing properties of sprayed antimony doped tin oxide thin films: solution molarity*, Journal of Alloys and Compounds **509**(6), 2011, pp. 3108–3115.
[33] BURSTEIN E., *Anomalous optical absorption limit in InSb*, Physical Review **93**(3), 1954, pp. 632–633.
[34] FREUND L.B., SURESH S., *Thin Film Materials: Stress, Defect Formation and Surface Evolution*, Cambridge University Press, Cambridge, 2003.
[35] LEE Y.H., LEE W.J., KWON Y.S., YEOM G.Y., YOON J.K., *Effects of CdS substrates on the physical properties of polycrystalline CdTe films*,Thin Solid Films **341**(1–2), 1999, pp. 172–175.
[36] MEMARIAN N., ROZATI S.M., ELEMURUGU E., FORTUNATO E., *Characterization of SnO_2:F thin films deposited by an economic spray pyrolysis technique*, Physica Status Solidi (C) **7**(9), 2010, pp. 2277–2281.
[37] IRIBARREN A., FERNÁNDEZ P., PIQUERAS J., *Influence of defects on cathodoluminescence along $ZnTe_xO_{1-x}$–ZnO microstructures grown by the vapour-solid technique*, Revista Cubana de Física **26**(2A), 2009, pp. 116–119.
[38] PEJOVA B., *The Urbach–Martienssen absorption tails in the optical spectra of semiconducting variable-sized zinc selenide and cadmium selenide quantum dots in thin film form*, Materials Chemistry and Physics **119**(3), 2010, pp. 367–376.
[39] MISHRA R.L., MISHRA S.K., PRAKASH S.G., *Optical and gas sensing characteristics of tin oxide nano-crystaline thin film*, Journal of Ovonic Research **5**(4), 2009, pp. 77–85.
[40] AKSOY S., CAGLAR Y., ILICAN S., CAGLAR M., *Effect of Sn dopants on the optical and electrical properties of ZnO films*, Optica Applicata **40**(1), 2010, pp. 7–14.
[41] FACHUN LAI, LIMEI LIN, RONGQUAN GAI, YONGZHONG LIN, ZHIGAO HUANG, *Determination of optical constants and thicknesses of In_2O_3:Sn films from transmittance data*, Thin Solid Films **515**(18), 2007, pp. 7387–7392.
[42] DEBAJYOTI D., RATNABALI B., *Properties of electron-beam-evaporated tin oxide films*, Thin Solid Films **147**(3), 1987, pp. 321–331.
[43] FANTINI M., TORRIANI I., *The compositional and structural properties of sprayed SnO_2:F thin films*, Thin Solid Films **138**(2), 1986, pp. 255–265.
[44] RAJPURE K.Y., KUSUMADE M.N., NEUMANN-SPALLART M.N., BHOSALE C.H., *Effect of Sb doping on properties of conductive spray deposited SnO_2 thin films*, Materials Chemistry and Physics **64**(3), 2000, pp. 184–188.
[45] FUJIWARA H., KONDO M., *Effects of carrier concentration on the dielectric function of ZnO:Ga and In_2O_3:Sn studied by spectroscopic ellipsometry: analysis of free-carrier and band-edge absorption*, Physical Review B **71**(7), 2005, article 075109.

[46] MERGEL D., QIAO Z., *Dielectric modelling of optical spectra of thin In_2O_3:Sn films*, Journal of Physics D: Applied Physics **35**(8), 2002, pp. 794–801.

[47] HODGSON J.N., *Optical Absorption and Dispersion in Solids*, Chapman and Hall, 1970.

[48] ILICAN S., ZOR M., CAGLAR Y., CAGLAR M., *Optical charecterization of the $CdZn(S_{1-x}Se_x)_2$ thin film deposited by spray pyrolysis method*, Optica Applicata **36**(1), 2006, pp. 29–37.

[49] TERRIER C., CHATELON J.P., ROGER J.A., BERJOAN R., DUBOIS C., *Analysis of antimony doping in tin oxide thin films obtained by the sol–gel method*, Journal of Sol–Gel Science and Technology **10**(1), 1997, pp. 75–81.

[50] YUNG-JEN LIN, CHING-JIUNN WU, *The properties of antimony-doped tin oxide thin films from the sol–gel process*, Surface and Coatings Technology **88**(1–3), 1997, pp. 239–247.

[51] IZERROUKEN M., KERMADI S., SOUAMI N., SARI A., BOUMAOUR M., *Influence of reactor neutrons irradiation on electrical, optical and structural properties of SnO_2 film prepared by sol–gel method*, Nuclear Instruments and Methods in Physics Research Section A **611**(1), 2009, pp. 14–17.

[52] YUHUA XIAO, SHIHUI GE, LI XI, YALU ZUO, XUEYUN ZHOU, BANGMIN ZHANG, LI ZHANG, CHENGXIAN LI, XIUFENG HAN, ZHENCHAO WEN, *Room temperature ferromagnetism of Mn-doped SnO_2 thin films fabricated by sol–gel method*, Applied Surface Science **254**(22), 2008, pp. 7459–7463.

[53] SHIEN A.R., KUBO A., DUFFY T.S., PRAKAPENKA V.B., SHEN G., *High-pressure phases in SnO_2 to 117 GPa*, Physical Review B **73**(1), 2006, article 014105.

[54] HAINES J., LEGÉR J.M., *X-ray diffraction study of the phase transitions and structural evolution of tin dioxide at high pressure: relationships between structure types and implications for other rutile-type dioxides*, Physical Review B **55**(17), 1997, pp. 11144–11154.

Received September 18, 2012
in revised form January 6, 2013